A Physical Model for the Transient Response of Capacitively Loaded Distributed *rlc* Interconnects

Raguraman Venkatesan, Jeffrey A. Davis and James D. Meindl

School of Electrical and Computer Engineering, Georgia Institute of Technology
791 Atlantic Drive NW, Atlanta, GA 30332-0269, USA
Phone: 1-404-894-9910 Fax: 1-404-894-0462 E-mail: vragu@ee.gatech.edu

ABSTRACT

Rapid approximation of the transient response of high-speed global interconnects is needed to estimate the time delay, crosstalk, and overshoot in a GSI multilevel wiring network. This paper outlines a rigorous and physical solution for transients in a capacitively-loaded distributed *rlc* interconnect using a convergent series of modified Bessel functions. Compact models for time delay and repeater insertion are derived. The single-line model is extended to evaluate crosstalk in two-coupled lines. These solutions are validated by HSPICE simulation, and have potential applications to rapid *rlc* timing analysis, global wire sizing and repeater insertion, signal integrity estimation, and reliability modeling (e.g. voltage overshoot and high current density concerns).

Categories and Subject Descriptors

B.4.3 [**Input/Output and Data Communications**]: Interconnections (Subsystems) – *physical structures (e.g. backplanes, cables, chip carriers).*

General Terms

Performance, Design, and Verification.

Keywords

Interconnects, distributed *rlc* lines, transient response, time delay, crosstalk, overshoot, repeaters.

1. INTRODUCTION

Being able to rapidly pinpoint interconnect noise and signal reliability problems caused by inductance in a GSI multilevel interconnect network is becoming extremely important for future multi-gigahertz systems. Direction of current research has focused on approximate models for the transient response of distributed *rlc* lines. For example, Ismail and Friedman used curve-fitted empirical models to extract expressions for time-delay of distributed *rlc* lines [7]. In addition Cao et al. [5] developed 2-pole and second order waveform models while Banerjee and Mehrotra [3], [4] used second and fourth order Pade approximations for the transfer function, the solutions of which require numerical iterations to calculate line characteristics such as time delay and crosstalk.

This paper focuses on models that describes transient waveforms on the state-of-the-art global interconnect structures that have one or two signal lines sandwiched between co-planar ground lines as in Fig. 1 [1], [8]. This paper significantly extends the work in [6] by rigorously solving the Laplace domain transfer function of a *capacitively loaded* distributed *rlc* line (Fig. 2) using a convergent series of modified Bessel functions to obtain a highly accurate and explicit solution for the transient response. These solutions are used to develop unified models for time delay and repeater insertion in *rc* and *rlc* interconnects. The complete model is extended to two-coupled lines, and the solutions are verified against HSPICE simulations.

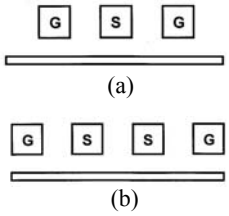

Fig 1. State-of-the-art global interconnect structures

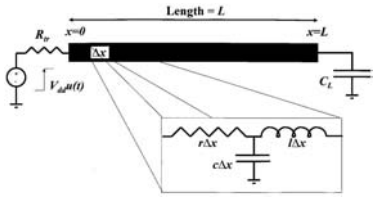

Fig 2. Distributed *rlc* line with load capacitance.

2. SINGLE LINE TRANSIENT MODEL

The voltage at the end of the line of length L, $V_{fin}(L,s)$, is described in the Laplace domain as [6]

$$V_{fin}(x=L,s) = (1+\Gamma_L)V_{inf}(L,s) + (1+\Gamma_L)\sum_{n=1}^{g}\left(\Gamma_L^n\Gamma_S^n V_{inf}\left((2n+1)L,s\right)\right) \quad (1)$$
$$= V_1(s) + V_2(s)$$

where n and g are the number of reflections, $V_{inf}(x,s)$ is the Laplace domain voltage at x for a distributed *rlc* line of infinite length given by

$$V_{inf}(x,s) = \frac{V_{dd}}{s}\frac{Z_o\sqrt{(s+r/l)/s}}{Z_o\sqrt{(s+r/l)/s}+R_{tr}}e^{-x\sqrt{lc}\sqrt{s(s+r/l)}}. \quad (2)$$

Γ_L and Γ_S are the reflection coefficients at the load and source ends respectively, defined as:

$$\Gamma_L = \frac{Z_L - Z(s)}{Z_L + Z(s)} = \frac{1 - sC_L Z_o\sqrt{1+\frac{r}{sl}}}{1 + sC_L Z_o\sqrt{1+\frac{r}{sl}}}, \quad \text{and} \quad \Gamma_S = \frac{Z_S - Z(s)}{Z_S + Z(s)} = \frac{R_{tr} - Z_o\sqrt{1+\frac{r}{sl}}}{R_{tr} + Z_o\sqrt{1+\frac{r}{sl}}} \quad (3)$$

DAC 2002, June 10-14, 2002, New Orleans, Louisiana, USA

where $Z_o = \sqrt{l/c}$ is the characteristic impedance of the line. The following two inverse laplace transform identities [9] will be used to obtain the time domain solution of (1) :

$$\left(\frac{s+\sqrt{s^2-\sigma^2}}{\sigma}\right)^{-v}\frac{e^{-k\sqrt{s^2-\sigma^2}}}{\sqrt{s^2-\sigma^2}} \rightarrow \left(\frac{t-k}{t+k}\right)^{\frac{v}{2}} I_v\left(\sigma\sqrt{t^2-k^2}\right)u_o(t-k), \quad v \geq 0 \tag{4}$$

where $I_v()$ is the modified Bessel function of order v.

$$\left(\frac{s+\sqrt{s^2-\sigma^2}}{\sigma}\right)^{v}\frac{e^{-k\sqrt{s^2-\sigma^2}}}{\sqrt{s^2-\sigma^2}} \rightarrow \left(\frac{t-k}{t+k}\right)^{\frac{v}{2}} I_v\left(\sigma\sqrt{t^2-k^2}\right)u_o(t-k) + 2\sum_{r=0}^{\left[\frac{v}{2}\right]}\sum_{m=0}^{\left[\frac{v}{2}\right]}\left[\begin{array}{l}\binom{v}{2m}\binom{2m-1}{2}{r}(-1)^r\sigma^{2r-v} \\ \times\left(\sum_{y=1}^{\left[\frac{v-2r-1}{2}\right]+1} C_{v-2r-1,y}\frac{\sigma^{v-2r-y+1}k t^{v-2r-2y+1}}{\left(\sqrt{t^2-k^2}\right)^{v-2r-y+1}} I_{v-2r-y+1}\left(\sigma\sqrt{t^2-k^2}\right)\right)\end{array}\right]u_o(t-k), \quad v>0 \tag{5}$$

where the coefficient $C_{x,y}$ is defined recursively as :

$$\begin{aligned} C_{x,y} &= 0 && y=0, \text{ for all } x \\ C_{x,y} &= 1 && x=0,\ y=1 \\ C_{x,y} &= 0 && x=0,\ y>1 \\ C_{x,y} &= (x-2y+3)C_{x-1,y-1} + C_{x-1,y} && \text{for all other x and y} \end{aligned} \tag{6}$$

i. First order reflection (n=0 or $t \leq 3t_f$)

Using algebraic expansions and inverse laplace transforms, the time domain solution for the first reflection (i.e. $t_f<t<3t_f$, t_f=time of flight) can be written as

$$V_{fin}(L,t_f<t<3t_f) = V_{DD}\frac{Z_o}{Z_o+R_{tr}}e^{\frac{-rt}{2l}} \times\left\{\begin{array}{l} P\sum_{i=0}^{\infty}(-M)^i\left(\frac{t-L\sqrt{lc}}{t+L\sqrt{lc}}\right)^{\frac{i+1}{2}} I_{i+1}\left(\sigma\sqrt{t^2-L^2lc}\right) \\ +Q\sum_{i=0}^{\infty}(-N)^i\left(\frac{t-L\sqrt{lc}}{t+L\sqrt{lc}}\right)^{\frac{i+1}{2}} I_{i+1}\left(\sigma\sqrt{t^2-L^2lc}\right) \\ +\frac{P}{1-G_s}\sum_{i=0}^{\infty}\sum_{k=1}^{\infty}(-M)^i\left(4-(1+G_s)^2G_s^{k-1}\right)\left(\frac{t-L\sqrt{lc}}{t+L\sqrt{lc}}\right)^{\frac{i+k+1}{2}} I_{i+k+1}\left(\sigma\sqrt{t^2-L^2lc}\right) \\ +\frac{Q}{1-G_s}\sum_{i=0}^{\infty}\sum_{k=1}^{\infty}(-N)^i\left(4-(1+G_s)^2G_s^{k-1}\right)\left(\frac{t-L\sqrt{lc}}{t+L\sqrt{lc}}\right)^{\frac{i+k+1}{2}} I_{i+k+1}\left(\sigma\sqrt{t^2-L^2lc}\right) \end{array}\right\} \times u_o\left(t-L\sqrt{lc}\right) \tag{7}$$

where

$$P=\frac{B\left(B+\sqrt{B^2+4}\right)}{\sqrt{B^2+4}}, \quad Q=\frac{-B\left(B-\sqrt{B^2+4}\right)}{\sqrt{B^2+4}}, \quad M=\frac{B+\sqrt{B^2+4}}{2}$$
$$N=\frac{B-\sqrt{B^2+4}}{2}, \quad B=\frac{4l}{rC_LZ_o}, \quad G_S=\frac{R_{tr}-Z_o}{R_{tr}+Z_o}, \quad \sigma=\frac{r}{2l} \tag{8}$$

When (7) no longer converges, a different set of algebraic expansions are used to write the first reflection laplace domain solution as

$$V_1'(s) = V_{DD}\frac{Z_o}{Z_o+R_{tr}}\frac{e^{-L\sqrt{lc}\sqrt{s^2-\sigma^2}}}{\sqrt{s^2-\sigma^2}} \left\{\begin{array}{l} \left(P\left(\sum_{i=0}^{\infty}M^{-i-1}(-1)^i\left(\frac{s+\sqrt{s^2-\sigma^2}}{\sigma}\right)^i\right)+Q\sum_{i=0}^{\infty}(-N)^i\left(\frac{s+\sqrt{s^2-\sigma^2}}{\sigma}\right)^{-i-1}\right) \\ \times\left(1+\frac{1}{1-G_s}\sum_{k=1}^{\infty}\left(\frac{s+\sqrt{s^2-\sigma^2}}{\sigma}\right)^{-k}\left(4-(1+G_s)^2G_s^{k-1}\right)\right) \end{array}\right\} \tag{9}$$

Using (4) and (5), the equivalent time domain solution can be written as $V_{fin}(L,t_f<t<3t_f) = e^{\frac{-rt}{2l}}V_1'(t), \quad V_1'(t) = L^{-1}\left[V_1'(s)\right]$ (10)

ii. Second and higher order reflections (n>0 or $t>3t_f$)

For second and higher order reflections (i.e. $t>3t_f$), the time domain solution can be written as

$$V_{fin}(L,t>3t_f) = e^{\frac{-rt}{2l}}V_{DD}\frac{Z_o}{Z_o+R_{tr}} \times\sum_{n=1}^{g}\left(\begin{array}{l} \left(S_C'+S_C''\right)\left(\frac{t-(2n+1)L\sqrt{lc}}{t+(2n+1)L\sqrt{lc}}\right)^{\frac{2i+2j+k+l+m+p+q+r}{2}} I_{2i+2j+k+l+m+p+q+r}\left(\sigma\sqrt{t^2-(2n+1)^2L^2lc}\right) \\ +\frac{1}{1-G_s}\left(S_C'+S_C''\right)\sum_{u=1}^{\infty}\left[\begin{array}{l} D\left(\frac{t-(2n+1)L\sqrt{lc}}{t+(2n+1)L\sqrt{lc}}\right)^{\frac{2i+2j+k+l+m+p+q+r+u}{2}} \\ \times I_{2i+2j+k+l+m+p+q+r+u}\left(\sigma\sqrt{t^2-(2n+1)^2L^2lc}\right)\end{array}\right] \\ \times u_o\left(t-(2n+1)L\sqrt{lc}\right)\end{array}\right) \tag{11}$$

where S_C' and S_C'' are notations used for compactness. They represent the following series summation functions :

$$S_C'\left(a^{-2i-2j-k-l-m-p-q-r}\right) = \sum_{i=0}^{n}\sum_{j=0}^{\infty}\sum_{k=0}^{\infty}\sum_{l=0}^{\infty}\sum_{m=0}^{n}\sum_{p=0}^{\infty}\sum_{q=0}^{n}\sum_{r=0}^{\infty}\left[\begin{array}{l}\frac{n(n+j-1)!}{i!\,j!(n-i)!}\frac{n(n+p-1)!}{m!\,p!(n-m)!}\frac{n(n-1+r)!}{q!\,r!(n-q)!}(-1)^{i+k+n+m+p+q} \\ \times\binom{-i}{k}\binom{-j}{l}B^{k+l+m+p}G_s^{n+r-q}a^{-2i-2j-k-l-m-p-q-r}\end{array}\right] \tag{12}$$

$$S_C''\left(a^{-2i-2j-k-l-m-p-q-r}\right) = \sum_{i=0}^{n+1}\sum_{j=0}^{\infty}\sum_{k=0}^{\infty}\sum_{l=0}^{\infty}\sum_{m=0}^{n}\sum_{p=0}^{\infty}\sum_{q=0}^{n}\sum_{r=0}^{\infty}\left[\begin{array}{l}\frac{(n+1)(n+j)!}{i!\,j!(n-i+1)!}\frac{(n+1)(n+p)!}{m!\,p!(n-m+1)!}\frac{n(n-1+r)!}{q!\,r!(n-q)!}(-1)^{i+k+n+m+p+q+1} \\ \times\binom{-i}{k}\binom{-j}{l}B^{k+l+m+p}G_s^{n+r-q}a^{-2i-2j-k-l-m-p-q-r}\end{array}\right] \tag{13}$$

$$\text{and, } D=4-\left(1+G_s\right)^2G_s^{k-1}, \quad a=\left(s+\sqrt{s^2-\sigma^2}\right)/\sigma\,. \tag{14}$$

When (11) no longer converges, a different set of algebraic expansions are used to write the laplace domain solution for higher order reflections as

$$V_2'(s) = \sum_{n=1}^{g}\left[\left(S_D'\left(a^{i+j-2m-p-q}\right)+S_D''\left(a^{i+j-2m-p-q}\right)\right)V_{inf}'\left((2n+1)L,s\right)\right] \tag{15}$$

where S_D' and S_D'' are the following functional notations used for compactness;

$$S_D'\left(a^{i+j-2m-p-q}\right) = \sum_{i=0}^{n}\sum_{j=0}^{\infty}\sum_{m=0}^{i+j}\sum_{p=0}^{n}\sum_{q=0}^{\infty}\left[\begin{array}{l}G_s^{n+q-p}\frac{n(n-1+j)!}{i!\,j!(n-i)!}\frac{n(n-1+q)!}{p!q!(n-p)!} \\ \times(-1)^{i+j+p+m}B^{-i-j}\binom{i+j}{m}a^{i+j-2m-p-q}\end{array}\right] \tag{16}$$

$$S_D''\left(a^{i+j-2m-p-q}\right) = \sum_{i=0}^{n+1}\sum_{j=0}^{\infty}\sum_{m=0}^{i+j}\sum_{p=0}^{n}\sum_{q=0}^{\infty}\left[\begin{array}{l}G_s^{n+q-p}\frac{(n+1)(n+j)!}{i!\,j!(n+1-i)!}\frac{n(n-1+q)!}{p!q!(n-p)!} \\ \times(-1)^{i+j+p+m}B^{-i-j}\binom{i+j}{m}a^{i+j-2m-p-q}\end{array}\right]. \tag{17}$$

Using (4) and (5), the corresponding time domain solution can be written as

$$V_{fin}(L,t>3t_f) = e^{\frac{-rt}{2l}}V_2'(t), \quad V_2'(t) = L^{-1}\left[V_2'(s)\right]. \tag{18}$$

iii. Comprehensive model

The comprehensive model consists of three separate models which are tabulated in Table I. The choice of model depends on conditions which are developed based on simple convergence rules applicable to summations of infinite series.

$$\text{Model 1 converges if } t \leq t_1, \text{ where } t_1 = \frac{64}{M\sigma}+t_f \tag{19}$$

while Model 2 converges if $t \le t_2$, where $t_2 = \frac{100}{11}\frac{2}{\mathrm{B}\sigma} + 3t_f$ (20)

Using (19) and (20), the comprehensive model can be described as in Table II. The comprehensive model is compared to HSPICE simulations for two values of the load capacitance in Fig. 3.

iv. Basis variables

Four dimensionless basis variables R_{ratio}, C_{ratio}, T_{ratio} and R_T, are defined as follows :

$$R_{ratio} = \frac{rL}{Z_o} = \frac{\text{line resistance}}{\text{characteristic impedance}},\quad C_{ratio} = \frac{C_L}{cL} = \frac{\text{load capacitance}}{\text{line capacitance}} \qquad (21)$$
$$T_{ratio} = \frac{t}{t_f} = \frac{\text{time}}{\text{time of flight}},\qquad R_T = \frac{R_{tr}}{Z_o} = \frac{\text{driver output resistance}}{\text{characteristic impedance}}$$

The complete transient model can be expressed in terms of just these 4 basis variables. These basis variables not only simplify the equations but also lend physical insight into the interplay of the various line parameters.

3. UNIFIED TIME DELAY MODEL

The 50% rise time t_d can be obtained by equating the transient voltage at the end of the line to $V_{DD}/2$. However, a simplified expression yields more physical insight and is therefore valuable. Using exponential series expansion, the 50% rise time in distributed *rlc* lines is simplified to

$$t_{d,ratio} = t_d / t_f = 1 + 0.693 C_{ratio}\left(R_{ratio} + 0.65R_T + 0.36\right) \quad (22)$$

Distinction between *rlc* lines (with considerable inductive effects) and *rc* lines (with dominant resistive effects) is achieved by evaluation of the following condition :

Condition I : "*If* $0.377R_{ratio} + 0.693R_T \le 1$, *use rlc models; else use rc models.*"

Therefore the *unified* time delay model for *rc* and *rlc* lines is :

$$t_{d,ratio} = t_d / t_f = \max\left(1,\ 0.377R_{ratio} + 0.693R_T\right) + 0.693C_{ratio}\left(R_{ratio} + 0.65R_T + 0.36\right) \quad (23)$$

The rise time in (23) can be interpreted as consisting of two parts: (a) time for the signal to reach the load end of the line and (b) time to charge up the load capacitance. The time for signal propagation through the interconnect is dictated by time-of-flight for *rlc* lines and by time to charge up the line capacitance in *rc* lines. Fig. 4 compares the model in (23) with the time delay calculated by HSPICE; for $0.1 \le R_{ratio} \le 5$, $0 \le C_{ratio} \le 0.1$ and $0.25 \le R_T \le 1$, the error is less than 2%.

4. OPTIMUM REPEATER INSERTION

Based on an analysis similar to that in [2], expressions for repeater insertion in *rlc* lines are derived. For an interconnect with k repeaters, each h times the size of a minimum feature-size repeater, the condition for quantitative differentiation between *rc* and *rlc* lines is

Condition II : "*If* $0.377R_{ratio}/k + 0.693R_T/h \le 1$, *use rlc models; else use rc models.*"

The unified expression for time delay is (Fig. 5)

$$t_{d,ratio} = t_d / t_f = \max\left(1,\ 0.377R_{ratio}/k + 0.693R_T/h\right) + 0.693C_{ratio}\left(hR_{ratio} + 0.65kR_T + 0.36\right). \quad (24)$$

Total time delay is minimized when each interconnect segment operates at time of flight (ToF) i.e. Condition II is satisfied in the equality for each segment – providing a relation between number and size of repeaters. Using this condition, the total time delay is minimized to calculate the optimum number (k_{opt}) and size of repeaters (h_{opt}) and optimum time delay ($t_{d,opt}$):

$$k_{opt} = 0.9513R_{ratio},\ h_{opt} = 1.208R_T \quad \text{and } t_{d\_opt,ratio} = t_{d\_opt}/t_f = 1 + 1.5532C_{ratio}R_{ratio}R_T \quad (25)$$

The equivalent *rc* optimal repeater expressions from [2] are:

$$k_{opt,rc} = \sqrt{(0.377R_{ratio})/(0.693R_TC_{ratio})},\ h_{opt,rc} = \sqrt{R_T/(R_{ratio}C_{ratio})} \quad (26)$$
$$\text{and } t_{d\_opt,ratio,rc} = 2.5\sqrt{C_{ratio}R_{ratio}R_T}$$

Using *rc* models for repeater insertion [2] may sometimes violate ToF operation, whereas *rlc* repeater models ensure compliance with ToF operation and do away with the excessive number of repeaters, resulting in a decrease in repeater count. Substituting (26) in Condition II gives the expression for differentiation between *rc* and *rlc* lines for optimum repeater insertion :

Condition III : "*If* $1.332\sqrt{R_{ratio}C_{ratio}R_T} \le 1$, *use optimum rlc models (25); else use optimum rc models (26).*"

The new models result in a fewer number of repeaters as well as smaller size of repeaters compared to [6] and [3], as can be seen from Fig. 6 and Fig. 7, decreasing total area needed for repeaters.

Table I. Composition of the 3 models

	$t \le 3t_f$	$t > 3t_f$
Model 1	Eqn (7)	Eqn (11)
Model 2	Eqn (10)	Eqn (11)
Model 3	Eqn (10)	Eqn (18)

Table II. Comprehensive model

	Comprehensive Model		
	For $t \le t_1$	For $t_1 \le t \le t_2$	For $t_2 < t$
If $t_1 < t_2$	Model 1	Model 2	Model 3
If $t_1 > t_2$	Model 1		Model 3

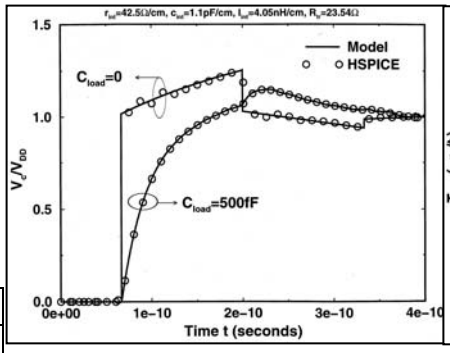

Fig 3. Transient response of a 1cm long interconnect - complete model vs HSPICE simulation.

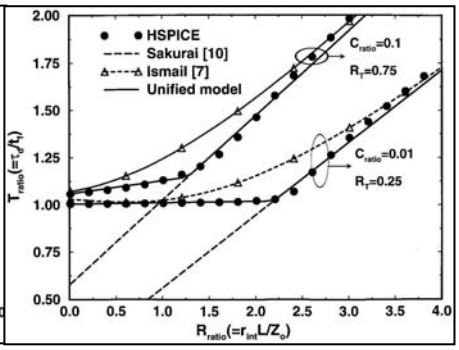

Fig. 4. Normalized time delay vs. R_{ratio} for different values of R_T and C_{ratio}.

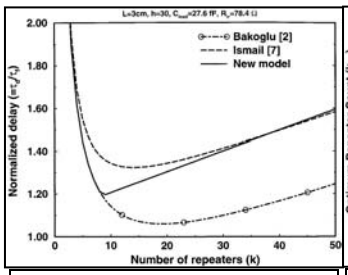

Fig. 5. Normalized delay vs. no. of repeaters, L=3 cm.

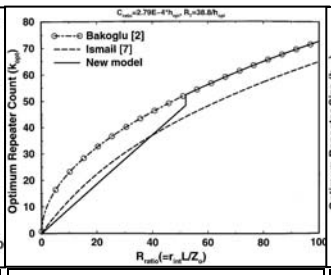

Fig. 6. Optimum number of repeaters vs line resistance.

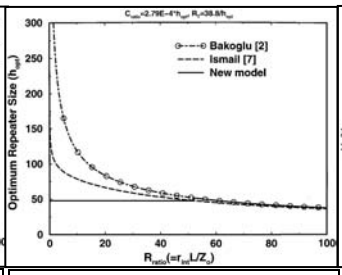

Fig. 7. Optimum size of repeaters vs line resistance.

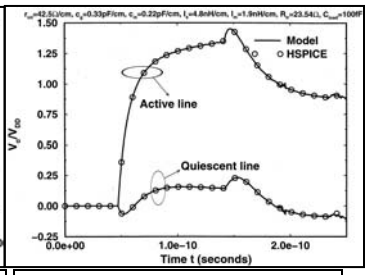

Fig. 8. Complete model vs HSPICE for 2-coupled lines.

5. CROSSTALK IN TWO COUPLED LINES

An important concern in high speed interconnect designs is the peak crosstalk induced in a quiescent line by an active neighbor (Fig 1 b). For two coupled lines, the transient voltage in the active and quiescent lines can be obtained based on an analysis similar to [6]. The differential equations describing signal propagation down two coupled lines is given by

$$\frac{\partial^2 \hat{V}}{\partial x^2} = r[C]\frac{\partial \hat{V}}{\partial t} + [L][C]\frac{\partial^2 \hat{V}}{\partial t^2}, \quad \hat{V} = \begin{bmatrix} V_A(x,t) \\ V_Q(x,t) \end{bmatrix} \tag{27}$$

The solutions for the active and quiescent line are given by

$$V_A(x,t) = 0.5[V_{fin}(r,\ l_s+l_m,\ c_g,x,t) + V_{fin}(r,\ l_s-l_m,\ c_g+2c_m,x,t)] \tag{28}$$

$$V_Q(x,t) = 0.5[V_{fin}(r,\ l_s+l_m,\ c_g,x,t) - V_{fin}(r,\ l_s-l_m,\ c_g+2c_m,x,t)] \tag{29}$$

where $V_A(x,t)$ and $V_Q(x,t)$ are the voltages at the end of the active and quiescent line. Fig. 8 compares the models in (28)–(29) with HSPICE simulations of the transient voltages in two-coupled lines. The presence of a load capacitor causes the peak crosstalk to occur after the second reflection (i.e. $t>3t_f$), whereas it occurs exactly at $t=3t_f$ in the no load case.The worst case time delay occurs when the two coupled lines are switching with opposite polarity; the transient response of the active line for the worst case time delay is

$$V_A(x,t) = V_{fin}(r,\ l_s-l_m,\ c_g+2c_m,x,t) \tag{30}$$

The worst case crosstalk occurs when both the lines are initially uncharged, and the active line charges to V_{DD}; the transient response of the quiescent line for the worst case crosstalk is given by (29). This two line solution is valid for ideal and non-ideal ground return paths because there are no constraints on the relation between the inductance and capacitance matrices.

6. PEAK OVERSHOOT

The single-line and two-coupled line transient expressions enable an easy and accurate calculation of the peak overshoot in the active line. Since the expressions are completely analytical, a fast and efficient algorithm can be used to compute the peak overshoot From Fig 3, it is clear that a larger load capacitance decreases peak overshoot.

7. COMPLETE MODEL VS HSPICE

HSPICE approximates a distributed rlc line by using large number of lumped elements, but at the expense of greater simulation time. The complete analytical model exactly solves the partial differential equation describing the interconnect system. The time stepping algorithm in HSPICE forces it to perform an exhaustive calculation of the transient response over a large range in order to pinpoint characteristics like time delay, crosstalk and overshoot. The ability of this new model to accurately calculate the transient response at an any time instant has the potential to utilize efficient algorithms to rapidly estimate desired interconnect characteristics.

8. CONCLUSIONS

A highly accurate and explicit solution has been rigorously derived for the transient response of single and two-coupled distributed *rlc* interconnects with a *capacitive load* termination. These solutions are validated by HSPICE simulation, and have been used to derive a unified model for rise time and repeater insertion. These new solutions have potential applications in CAD for rapid timing analysis, global wire sizing and repeater insertion, signal integrity estimation, and reliability modeling (e.g. voltage overshoot and high current density concerns).

9. REFERENCES

[1] F.E.Anderson, J.S.Wills and E.Z.Berta, "The core clock system on the next generation Itanium microprocessor," in Proc. of ISSCC, pp. 146-147, 2002.

[2] H.B.Bakoglu, "Circuits, interconnections and packaging for VLSI," Reading, MA: Addison Wesley, 1990.

[3] K.Banerjee and A. Mehrotra, "Analysis of on chip inductance effects using a novel performance optimization methodology for distributed RLC interconnects", in Proc. of DAC, pp.798-803, 2001.

[4] K.Banerjee and A. Mehrotra, "Accurate analysis of on chip inductance effects and implications for optimal repeater insertion and technology scaling," in Proc. of symposium on VLSI circuits, pp. 195-198, 2001.

[5] Y.Cao, X.Huang, D.Sylvester and C.Hu, "A new analytical delay and noise model for on-chip *RLC* interconnect," Proc. of IEDM, pp. 823-826, Dec. 2000.

[6] J.A.Davis and J.D.Meindl, "Compact distributed *rlc* interconnect models - Part I: Single line transient, time delay and overshoot expressions," IEEE Trans. Elect. Dev., Nov 2000, pp. 2068-2077.

[7] Y.I.Ismail and E.G.Friedman, "Effects of inductance on the propagation delay and repeater insertion in VLSI circuits," IEEE Trans. VLSI Sys., Apr 2000, pp.195-206.

[8] A.Kowalczyk et al., "First generation MAJC dual microprocessor," in Proc. of ISSCC, pp. 236-237, 2001.

[9] G.E.Roberts and H.Kaufman, *Table of Laplace Transforms,* W.B.Saunders Company, 1966.

[10] T.Sakurai, "Closed form expressions for interconnect delay, coupling and crosstalk," TED, Jan 1993, pp. 118-124.